

**AN IMPROVED METHOD FOR ASTEROID IMPACT PROBABILITY DUE TO SWARM INTELLIGENCE ALGORITHMS** Andrew D. Koehler<sup>1</sup>, Bruce A. Conway<sup>1</sup>, <sup>1</sup>University of Illinois Urbana-Champaign, Urbana, Illinois, 61801, USA; adkoehl2@illinois.edu, bconway@illinois.edu;

**Keywords:** *earth-asteroid minimum close approach distance, particle swarm optimization*

**Introduction:** Given the vast number of asteroids and comets in the Solar System, there is a self-preservation imperative to be vigilant about discovering and tracking asteroids and comets and determining whether or not they are on an Earth-impacting trajectory. This research explores two fundamental questions regarding the orbital dynamics of potentially hazardous objects (PHOs): (1) given the best orbit determination solution, i.e. a state and uncertainty at a specific time, what is the closest that asteroid ever gets to the Earth when propagated forwards in time? and (2) how can the computationally expensive process of running a Monte Carlo simulation, with potentially thousands or millions of samples, be improved?

This paper introduces an improved method for the determination of Earth close approach minimum distances of potentially hazardous asteroids and comets. Inspired by recent advancements in swarm intelligence (SI), this novel method characterizes the set of possible perigees and finds the minimum Earth close approach distance by posing the asteroid close approach (CA) problem as a trajectory optimization problem, wherein a modified Particle Swarm Optimization (PSO) implementation is used to find the smallest possible perigee for the PHO given its current best known mean orbit and the 3-sigma uncertainty bounds for all its orbital elements. Belonging to the class of swarm intelligence, PSO is a numerical optimization method inspired by the collective behavior of a flock of birds, school of fish, swarm of insects, or other creatures in search of food or escape from predators. With this new method, the classic Monte Carlo algorithm can be reframed as a “zeroth-order” swarm intelligence algorithm. Given a swarm’s ability to share information between particles and move closer to the objective from one iteration to the next, improvement upon traditional methods is guaranteed. The novel method is applied in case studies on the asteroids Apophis and Bennu and the comet Swift-Tuttle.

**Literature Review:** Researchers have been studying the risk of potential impact by asteroids and comets for decades. This literature review focuses on the orbital dynamics of potentially hazardous objects, including methods of determining the Earth close approach nominal and mini-

imum distances of such objects and predictions regarding their probability of impact with the Earth. Apophis is the most thoroughly studied potentially hazardous asteroid, and its threat provided serious motivation to researchers attempting to better understand PHO impact probability. Chesley et al. used a line of variations (LOV) approach to analyze the Apophis 2029 and 2036 close encounters [1]. In this approach, a one-dimensional continuous line (the major axis of the confidence ellipsoid, assuming the confidence region is well represented by the confidence ellipsoid) is sampled rather than the orbital state’s entire six-dimensional confidence region. Giorgini et al. analyzed the Earth close encounters of Apophis by calculating the asteroid’s close approach minimum distances via Monte Carlo (MC) simulation with sample size  $N_m = 10,000$  [2], determining a minimum distance of 0.000244 AU during its 2029 close approach (CA) with Earth. Milani et al. also analyzed the impact risk of Apophis with the LOV and MC approach, using up to 1 million samples in their MC simulations [3]. In particular, Milani discusses the difficulties of using a computationally expensive MC method, often with many thousands of virtual asteroids (VA), to try and find those that become virtual impactors (VI). The MC method will more thoroughly sample the confidence region compared to the more efficient yet less exhaustive LOV method. This research is motivated by the need for a thorough yet more efficient approach to the PHO close approach problem.

In the context of trajectory optimization, direct methods formulate the optimization problem based on physically meaningful system parameters, e.g. thrust magnitude and direction, time of flight, orbital parameters, etc. [4]. A further classification of direct methods can be made, differentiating between deterministic and stochastic methods. A deterministic method requires continuity, differentiability of the objective function to be minimized, and often a satisfactory initial guess that can lead to convergence on a solution. Because of the challenges associated with such techniques, it is desirable to pursue stochastic methods which require no knowledge of the derivatives nor reasonable first-order solutions, making them adept at solving problems with as little information *a priori* as possible. Numerous researchers have explored the use of stochastic optimization methods, includ-

ing nature-inspired evolutionary and swarm algorithms. Swarm intelligence methods were introduced in 1993 by Beni and Wang [5]. Pontani and Conway demonstrated the effectiveness of applying Particle Swarm Optimization to solve several types of spacecraft trajectory optimization problems, including the determination of Lyapunov period orbits and the optimal thrust pointing-angle-time-history for a minimum time of flight optimal low-thrust transfer from Earth to Mars [6].

**Methodology:** This paper focuses on the orbital dynamics of potentially hazardous objects, including a framework for the gravitational equations of motion in two propagation segments: first, a Sun-centered dynamics model where the PHO is in a closed, elliptical orbit, and second, an Earth-centered dynamics model (including the J2 perturbation due to the Earth’s oblateness), where the PHO is on an open, hyperbolic trajectory. Ephemerides from the NASA JPL NAIF SPICE Toolkit are used to compute third-body perturbations due to the 8 major planets and Pluto, Ceres, Pallas, and Vesta and the PHO-Earth close approach distance.

The PHO close approach problem is posed as a trajectory optimization problem, with a cost function  $J$  equal to the perigee distance of the virtual asteroid (or comet) trajectory.

$$J = r_p = \left[ r_x^2(t_p) + r_y^2(t_p) + r_z^2(t_p) \right]^{1/2} \quad (1)$$

This objective function incentivizes the optimizer to try and find the smallest possible Earth close approach minimum distance. The decision variables for the optimizer are defined as the orbital elements (semi-major axis, eccentricity, inclination, right ascension of the ascending node, argument of perapsis, and mean anomaly) at some initial epoch  $t_0$ .

$$\mathbf{x} = [a \ e \ i \ \Omega \ \omega \ M] \quad (2)$$

The upper and lower bounds are defined at  $\pm 3\sigma$ , where  $\sigma$  is one standard deviation in the uncertainty of the orbit element, assuming a Gaussian distribution.

$$\begin{aligned} \mathbf{x}_{\text{ub}} &= 3 [\sigma_a \ \sigma_e \ \sigma_i \ \sigma_\Omega \ \sigma_\omega \ \sigma_M] \\ \mathbf{x}_{\text{lb}} &= -3 [\sigma_a \ \sigma_e \ \sigma_i \ \sigma_\Omega \ \sigma_\omega \ \sigma_M] \end{aligned} \quad (3)$$

In order to determine the close approach minimum distance of a potentially hazardous asteroid, a sufficiently representative dynamics model must be used. The dynamic framework includes two propagation segments: first, a Sun-centered dynamics model where the PHO is in a closed, elliptical orbit, and second, an Earth-centered dynamics model, where the asteroid is on an open, hyperbolic orbit. The simulation begins with a PHO in orbit about the Sun, with perturbing accelerations from all 8 planets (Mercury, Venus, Earth, Mars, Jupiter, Saturn, Uranus, and Neptune), the Earth’s Moon, two dwarf planets (Pluto and Ceres), and two asteroids (Pallas and Vesta). According to Giorgini et. al, these are the 13 planetary bodies with the most significant gravitational perturbations on the asteroid Apophis [2]. This analysis does not include non-gravitational perturbations such as solar radiation pressure (SRP), the Yarkovsky effect, relativistic effects, or atmospheric drag. The Yarkovsky effect is a significant source of perturbation (in particular compared to SRP), and it depends on several unknown asteroid parameters including shape, spin rate, and spin axis. Assumptions about the nature of the unknown asteroid parameters could be made, however, reasonable uncertainty values would extend beyond the perceptible effects of the perturbations. The NASA JPL NAIF “SPICE” Toolkit is used for planetary ephemeris data when calculating third-body perturbations [7], [8]. The planetary position vectors in this work come from the most up-to-date planetary ephemeris model, de440.bsp, generated by fitting ground and space-based observations to the numerically integrated orbits of all planetary bodies in the Solar System [9].

A proper method of orbit simulation must be programmed accurately and efficiently simulate the dynamics of the PHO close approach with Earth. This effort employs use of one of the most straightforward special perturbation methods: Cowell’s method, first used by Cowell and Crommelin for determining the orbit of Halley’s comet and predicting the time of its 1910 perihelion passage and corresponding orbital elements as accurately as possible [10]. Using Cowell’s method, the equations of motion for body  $i$  in a heliocentric ecliptic J2000 frame with third-body perturbations from 13 planetary bodies can be written as follows in Equation 4

$$\ddot{\mathbf{r}}_i = -\frac{\mu_\odot \mathbf{r}_i}{r_i^3} + \sum_{j=1}^{n=13} -\mu_j \left( \frac{\mathbf{r}_i - \mathbf{r}_j}{\|\mathbf{r}_i - \mathbf{r}_j\|^3} + \frac{\mathbf{r}_j}{r_j^3} \right) \quad (4)$$

where  $i$  denotes the body of interest (in this case, a PHO),  $j$  denotes one of the thirteen third-body perturbers,  $\ddot{\mathbf{r}}$  denotes the acceleration vector,  $\mathbf{r}$  denotes the position vector from the origin (the Sun) to the specified body, and  $\mu$  corresponds to the standard gravitational parameter of a given planetary body. The virtual asteroid trajectories move

from a Sun-centered propagation to an Earth-centered propagation when they enter the Earth's sphere of influence (SOI), calculated using the following approximation from Prussing and Conway [11]

$$r_{SOI} = \left( \frac{m_p}{m_s} \right)^{2/5} r_{sp} \quad (5)$$

where  $m_p$  is the mass of the planet (in this case, the Earth),  $m_s$  is the mass of the Sun, and  $r_{sp}$  is the distance from the Sun to the planet. Once the asteroid reaches the Earth SOI, the state is converted from the heliocentric ecliptic J2000 frame to the geocentric ecliptic J2000, as specified in Equation 6

$$\mathbf{r}_{\oplus i} = \mathbf{r}_{\odot i} - \mathbf{r}_{\odot \oplus} \quad (6)$$

where astronomical symbols are used for the Earth ( $\oplus$ ) and Sun ( $\odot$ ). Next, Cowell's method is again employed in the Earth-centered dynamics model, as detailed in Equation 7.

$$\ddot{\mathbf{r}}_i = -\frac{\mu_{\oplus} \mathbf{r}_i}{r_i^3} + \sum_{j=1}^{n=2} -\mu_j \left( \frac{\mathbf{r}_i - \mathbf{r}_j}{\|\mathbf{r}_i - \mathbf{r}_j\|^3} + \frac{\mathbf{r}_j}{r_j^3} \right) + \mathbf{a}_{J_2} \quad (7)$$

An additional perturbation included in the Earth-centered propagation is the  $J_2$  perturbation due to the oblateness of the Earth, where the perturbing acceleration is determined by Equation 8 from Prussing and Conway.

$$\mathbf{a}_{J_2} = \frac{-3\mu J_2 R_{\oplus}^2}{r^4} \left[ \hat{\mathbf{e}}_R \left( \frac{1}{2} - \frac{3 \sin^2 i \sin^2 \theta}{2} \right) + \hat{\mathbf{e}}_T \sin^2 i \sin \theta \cos \theta + \hat{\mathbf{e}}_N \sin i \sin \theta \cos i \right] \quad (8)$$

Modern Monte Carlo statistical methods have been a fundamental component of science and engineering analyses since Metropolis, Ulam, et al. [12], in particular when determining likely outcomes of a system with parameters with some estimated probability distribution. For the Earth Close Approach problem, a Monte Carlo simulation is implemented, where a set of ten thousand random uniformly distributed initial orbital elements are generated, and then each of the initial states is propagated forward in time to see if there is a risk of collision with the Earth.

Particle Swarm Optimization was created by Kennedy and Eberhart in 1995 [13]. The PSO method begins by generating a random initial population according to some distribution, typically normal or uniform. Each particle in the population has an associated position vector for its location

in the search-space of feasible solutions of the  $n$  dimensional optimization problem. Each iteration updates the position with a velocity vector based upon three components with associated weighting coefficients: inertial, cognitive, and social. The inertial component biases each particle to continue moving in the direction it was moving in during the previous iteration. The cognitive component biases the particle to move towards the best position that it has experienced, i.e. towards its personal best fitness. The social component biases the velocity towards the global best fitness found by any particle in the population. It is important to have sufficient number of particles  $N_p$  such that the swarm is resilient to a poor initial guess, i.e. the exploratory nature of PSO allows it to perform global optimization well without a good initial guess.

The MATLAB computing language was used for numerical computation for this paper [14]. The MATLAB built-in function `ode113`, a variable-step, variable-order (VSVO) Adams-Bashforth-Moulton Predict-Evaluate-Correct-Evaluate (PECE) solver [15], was used to integrate the equations of motion. This specific ode solver was chosen to solve the initial value problem for the ordinary differential equations expressed in Equations 4 and 7 because it is more efficient at solving problems with stringent error tolerances and relatively expensive ODE functions, which is particularly useful for this high-accuracy, high-fidelity orbital dynamics simulation. Table 1 below shows options used for the `ode113` function.

**Table 1: MATLAB `ode113` options**

Option	Value
Relative Error Tolerance	1e-13
Absolute Error Tolerance	1e-14
Event1 value	$\frac{d}{dt} \ \mathbf{r}_i - \mathbf{r}_{\oplus}\ $
Event1 isterminal	0 (False)
Event1 direction	1 (increasing)
Event2 value	$\ \mathbf{r}_i - \mathbf{r}_{\oplus}\  - r_{SOI}$
Event2 isterminal	1 (True)
Event2 direction	-1 (decreasing)

**Case Study I) 99942 Apophis:** The first case study focuses on 99942 Apophis, an Aten class (Earth-crossers with a semi-major axis less than 1 AU and perihelion greater than 0.983 AU) potentially hazardous asteroid (PHA). Table 2 shows orbital elements for Apophis on 01-Jan-2024 12:00:00 TDB. The  $1\sigma$  uncertainty values are

representative for a newly discovered PHO. In this simulation, the virtual asteroids are generated by randomly sampling from the orbit state and uncertainty detailed in Table 2 and then propagated five and a half years until Earth close approach on 13-Apr-2029.

**Table 2: Apophis Orbital Elements at Epoch 01-Jan-2024 12:00:00 TDB**

Element	Value	Uncertainty ( $1\sigma$ )	Units
$e$	0.1914	9.208e-7	-
$a$	1.3804e8	37.782	km
$i$	3.339	1.840e-6	deg
$\Omega$	203.957	1.759e-3	deg
$\omega$	126.601	2.654e-3	deg
$M$	265.731	7.192e-4	deg

Tables 3 and 4 show relevant parameters for the MC and PSO methods for this simulation.

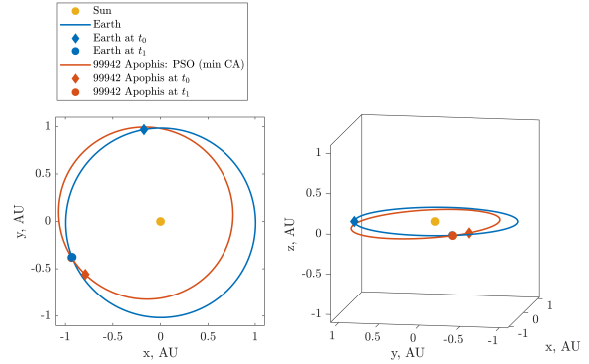
**Table 3: MC options - Apophis Case Study**

Option	Value
random distribution type	Normal (Gaussian)
number of virtual asteroids	10,000
z-score	3

**Table 4: PSO options - Apophis Case Study**

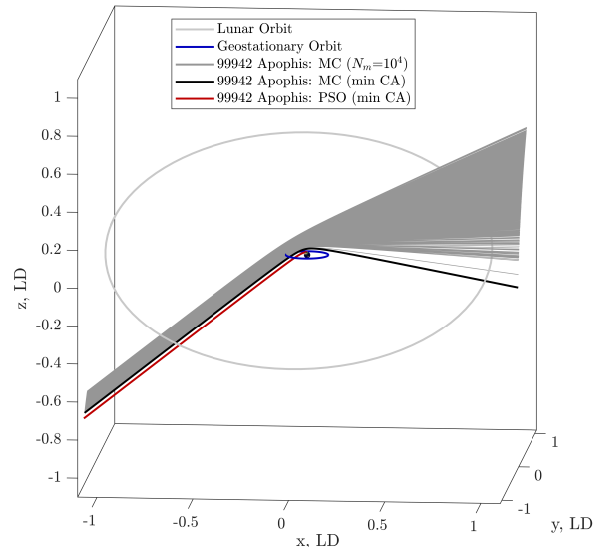
Option	Value
random distribution type	Uniform
number of virtual asteroids	1000
number of generations	10
search space boundary	$\pm 3\sigma$
inertial weight coefficient	0.65
cognitive acceleration coefficient	2
social acceleration coefficient	2
maximum velocity	14.7
boundary switch	slide

Figure 1 shows the optimal asteroid trajectory (with the minimum close approach distance to the Earth) from PSO alongside the Earth's path in the Sun-centered ecliptic J2000 frame. Figure 2 shows the asteroid trajectories as they enter the Earth Sphere of Influence (SOI). The orbit of the Moon is shown in light gray and geostationary orbit is shown in dark blue. The virtual asteroid trajectories are inbound from the left side of the figure (below the ecliptic plane) and pass by the Earth at the



**Figure 1: Asteroid 99942 Apophis trajectories, Heliocentric Ecliptic J2000 frame**

ascending node. The minimum close approach trajectory from MC is shown in black. The effect of the Earth flyby can be clearly seen in the expansion of the gray band of trajectories, with the black minimum close approach trajectory having the greatest turn angle and thus rotation of its  $v_\infty$  vector. The optimal trajectory from PSO (shown in red) is an Earth impactor trajectory. Figure 3 shows a closer



**Figure 2: Asteroid 99942 Apophis trajectories, Geocentric Ecliptic J2000 frame [ $\sim 1$  LD]**

view of the geocentric ecliptic frame, highlighting the significant gap between the minimum close approach trajectory from MC and the Earth impactor trajectory found using PSO. The orientation of the Earth corresponds to the approximate time the asteroid would enter Earth's atmosphere. Figure 4 shows the projection onto the classic "B-Plane" as well as the "A-Plane" (A for closest Approach),

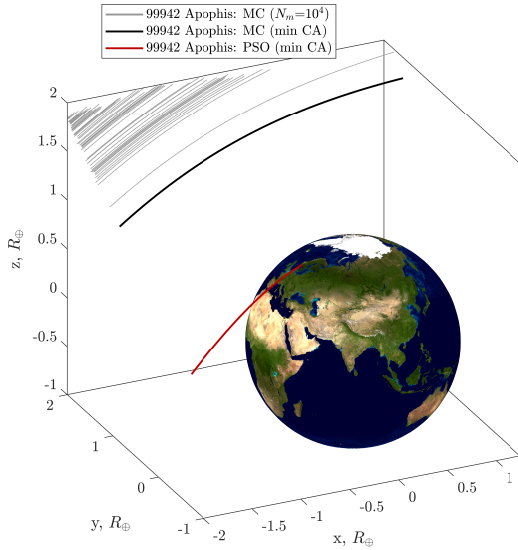


**Figure 3: Asteroid 99942 Apophis trajectories, Geocentric Ecliptic J2000 frame [ $\sim 1 R_{\oplus}$ ]**

which instead of using the inbound  $v_{\infty}$  vector to define the direction orthogonal to the plane, it uses the velocity at periapsis  $v_p$  (this has also been referred to as the Modified target plane [3]). The key result is that the A-Plane crossing shows a virtual impactor found by PSO, whereas the closest MC virtual asteroid is thousands of km from the Earth.

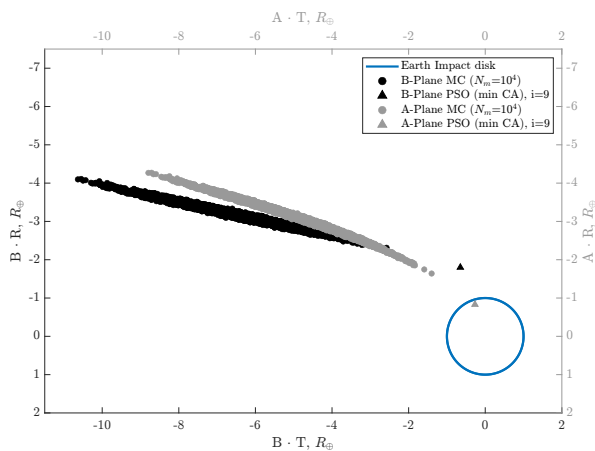


**Figure 4: Asteroid 99942 Apophis A-Plane and B-Plane crossing**

Figure 5 shows a scatter plot of the perigees of all the virtual asteroid trajectories. The y-axis has units Earth radii, with the black line being drawn at  $1R_{\oplus}$  to mark the Earth impactor boundary (a trajectory below that line would hit the Earth - assum-

ing a spherical Earth with radius  $R_{\oplus} = 6378.137$  km). The x-axis is normalized such that the origin is the time of perigee of the PSO minimum close approach trajectory. This figure, along with the following Figure 6 clearly illustrate the movement of PSO particles towards the minimum close approach distance. On the first iteration (shown in blue), the swarm’s movement is in the right direction. By iteration 9 (shown in orange), the particles have converged onto the global minimum.

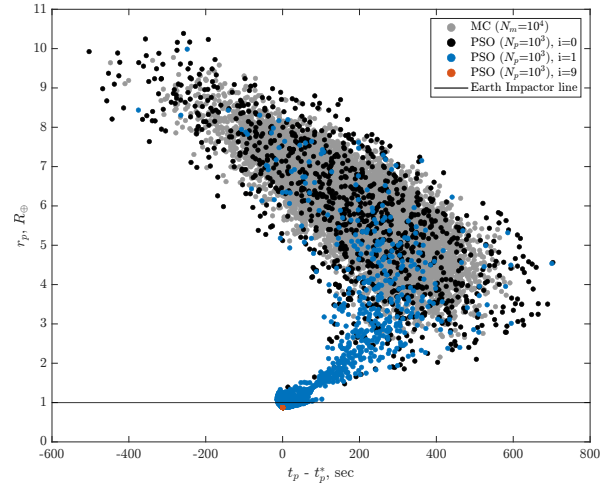


**Figure 5: Asteroid 99942 Apophis Minimum Distances from Earth’s center,  $t_p^* = 13\text{-Apr-2029 21:42:32 UTC}$**

Figure 6 shows the population of initial conditions for MC (a normal distribution) and several iterations of PSO as the particles move towards the minimum close approach distance. The PHO initial orbital elements  $a, e, i, \Omega, \omega, M$  are shown on the x-axes, which are normalized to be in units of  $\sigma$ , where  $1\sigma$  corresponds to a single standard deviation from the mean  $\mu$ . The minimum close approach distance in units of Earth radii is shown on the y-axis. A black line is drawn again at one Earth radii. Four sets of initial conditions are shown for each of the six orbital elements: (1) the random Monte Carlo samples, (2) the random zeroth generation of PSO, (3) the first generation of PSO that finds an Earth impactor, and (4) the final generation of PSO. Neither the Monte Carlo initial population nor the PSO initial population (zeroth iteration  $i = 0$ ) detect an Earth impactor trajectory. On just the first iteration, PSO finds several initial conditions that result in an Earth impactor trajectory. By the tenth iteration, nearly the entire PSO population converges to below the Earth impactor boundary.

The initial semi-major axis that results in the minimum close approach distance is when  $a$  is three standard deviations less than the mean. On the first iteration of PSO, the swarm has moved towards  $a - \mu = -3\sigma$ . At the tenth iteration, the PSO swarm has concentrated onto the global best solution at  $-3\sigma$ . Earth impactor trajectories are only possible if the semi-major axis is significantly overestimated by the orbit determination (OD) solution.

The initial eccentricity space has initial conditions that result in Earth impactor trajectories throughout  $(e - \mu)/\sigma \in [-3, -1]$ . There are no impactors found if  $(e - \mu)/\sigma > -1$ .

The initial inclination space has initial conditions that result in Earth impactor trajectories throughout  $(e - \mu)/\sigma \in [-3, 3]$ . There are initial inclinations below, near, and above the mean estimated value that all can result in Earth impactor trajectories.

For both right ascension of the ascending node and argument of periaapsis, the minimum close approach distance is when  $\Omega$  and  $\omega$  are three standard deviations greater than the mean. Earth impactor trajectories are only possible if  $\Omega$  is significantly underestimated by the OD solution.

The mean anomaly at the initial epoch that results in the minimum close approach distance is when  $M$  is three standard deviations greater than the mean. Similar to  $\Omega$  and  $\omega$ , Earth impactor trajectories are only possible if  $M$  is significantly underestimated by the OD solution. Since this Apophis-like PHO has an inclination of 3.34 deg with respect to the ecliptic plane, an impact with the Earth can only occur at one of the nodes (in the case of the 2029 Earth flyby it is the ascending node). In summary, the initial orbital element space is thoroughly explored with the PSO method, characterizing if Earth impacting trajectories are feasible given the current best OD estimate of the PHO state.

The PHO minimum close approach distances for the Apophis case study are shown in Table 5. The difference between the minimum CA found on iteration zero highlights the importance of using a uniformly distributed initial population instead of a normal one (even when the normal population benefits from ten times the sample size). The effectiveness of PSO is clear since it finds previously undiscovered minimum CA distances in only a few iterations. In addition, PSO proves to be more efficient at determining the minimum close approach distance since it finds Earth impactors in two thousand function evaluations (numerically integrating the asteroid state after the initial random sampling) that MC could not find in ten thousand.

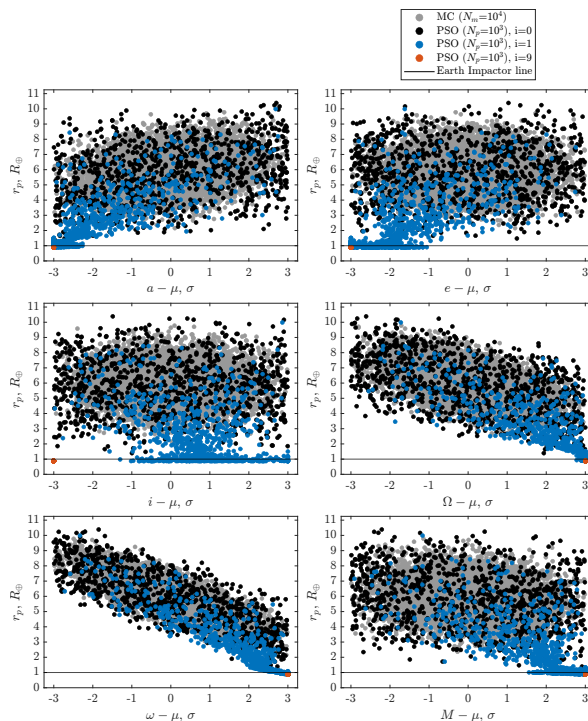


Figure 6: Asteroid 99942 Apophis Initial Conditions

Table 5: Minimum Close Approach Distances, Apophis Case Study

Method	Iteration	Minimum CA, $R_{\oplus}$
MC	0	2.15625
PSO	0	1.38789
	1	0.87357
	2-9	0.87351

**Case Study II) 101955 Bennu:** The second case study focuses on 101955 Bennu, an Apollo class (Earth-crossers with a semi-major axis greater than 1 AU and perihelion less than 1.017 AU) potentially hazardous asteroid. Table 6 shows orbital elements for Bennu on 01-Jan-2130 12:00:00 TDB. The  $1\sigma$  uncertainty values are representative for a newly discovered PHO. In this simulation, the virtual asteroids are generated by randomly sampling from the orbit state and uncertainty detailed in Table 6 and then propagated five years through the Earth close approach on 25-Sep-2135. The simulation continues to run for another 48 years after the first Earth close approach in order to see if any of the virtual asteroids make a second close approach with Earth. This case study focuses on the comparison between MC and PSO for a “keyhole” analysis,

i.e. when a PHO has a possible second close approach of Earth after its initial close approach. In this scenario, the PSO objective function is set to minimize the second minimum close approach distance (with no weight given to the first minimum close approach distance). For the Bennu case

**Table 6: Bennu Orbital Elements at Epoch 01-Jan-2130 12:00:00 TDB**

Element	Value	Uncertainty ( $1\sigma$ )	Units
$e$	0.1973	2.6156e-08	-
$a$	1.6613e8	11.036	km
$i$	6.244	2.573e-6	deg
$\Omega$	0.352	2.084e-5	deg
$\omega$	70.662	2.416e-5	deg
$M$	346.655	1.603e-5	deg

study, the number of samples for MC is set to 1,000 while the population of PSO is set to 10 particles and 25 generations (all other MC and PSO options are kept the same). Figure 7 shows the optimal asteroid trajectory (with the minimum close approach distance to the Earth) from PSO alongside the Earth’s path in the Sun-centered ecliptic J2000 frame.

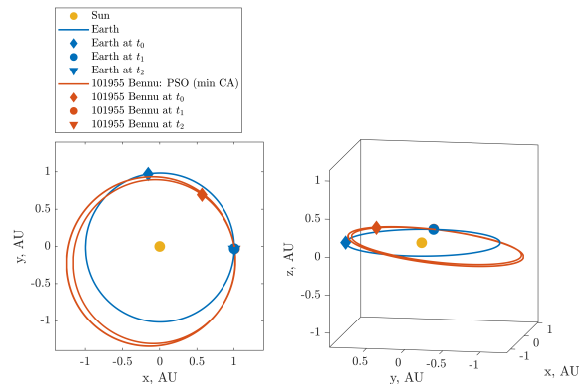


**Figure 7: Asteroid 101955 Bennu Close Approaches, Heliocentric Ecliptic J2000 frame**

The two sets of Bennu close approaches are shown in the A-Plane in Figure 8. The first set of close approaches that occur on 25-Sep-2135 are shown in black in subplot III, and the second set of close approaches are shown in gray. The keyhole, i.e. a point on the A-Plane that results in an Earth impact on the following close approach, is at the right edge (and closest to Earth) of the dispersion of initial close approaches. This case study further demonstrates the effectiveness of the

PSO method for the PHO close approach problem, especially in a keyhole situation where multiple close approaches are expected. PSO finds an Earth impactor on the second close approach with a population of only 10 particles and 25 iterations, whereas the 1,000 sample MC simulation has a minimum second close approach distance exterior the Earth’s sphere of influence.

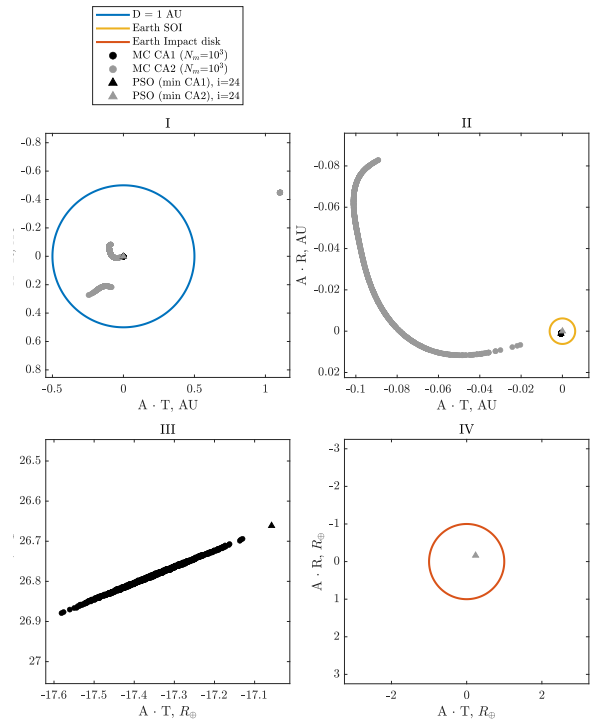


**Figure 8: Asteroid 101955 Bennu A-Plane crossing**

In the Bennu keyhole analysis case study, the close approaches are plotted with a logarithmic y-axis since the second set of close approaches vary widely. In Figure 9, the PSO particles quickly swarm down the “funnel” shape outlined by the MC and PSO initial populations. Figure 10 shows the population of initial conditions for MC and three iterations (initial, first impact detection, and final) of PSO as the particles move towards the minimum second close approach distance. On the fourth iteration, PSO finds a set of initial conditions that result in an Earth impactor trajectory. By the 24th iteration, PSO has found multiple sets of initial conditions that lead to an Earth impact. The PSO particles find Earth impactors for semi-major axes and eccentricities at  $3\sigma$  below the mean, for inclinations  $\in [-2, -1]\sigma$ , for right ascension of the ascending nodes near  $2.6\sigma$ , and for argument of periapsis and mean anomaly at  $3\sigma$  above the mean. In sum-

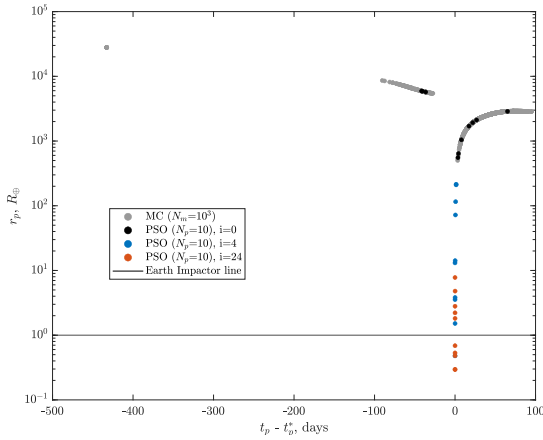


**Figure 9: Asteroid 101955 Bennu Minimum Distances from Earth's center**

mary, the initial orbital element space is thoroughly explored with the PSO method, characterizing if Earth impacting trajectories upon second close approach are feasible given the current best OD estimate of the PHO state. A challenge of the keyhole analysis approach is that the PHO orbit determination solution will be improved and the uncertainty reduced during the first close approach. However, it still remains a prudent strategy for analyzing the feasibility of future impacts following an PHO-Earth close approach.

The PHO minimum close approach distances for the Bennu case study are shown in Table 7.

The effectiveness of PSO is clear since it finds previously undiscovered minimum CA distances in only a few iterations. In addition, PSO proves to be more efficient at determining the minimum close approach distance since it finds Earth impactors in two hundred and fifty function evaluations that MC did not find in one thousand.

**Case Study III) Comet Swift-Tuttle:** The third case study focuses on the comet 1000140 109P Swift-Tuttle, a Halley-type (periodic between 20 and 200 years) potentially hazardous comet. Table 8 shows orbital elements for Swift-Tuttle on 10-Oct-1995 00:00:00 TDB. The  $1\sigma$  uncertainty values are representative for a newly discovered PHO (with a relatively short data arc). In this simulation, the virtual comets are generated by randomly sampling from the orbit state and uncertainty detailed in Table 8 and then propagated 131 years through the Earth close approach on 14-Aug-2126. In this scenario, the PSO objective function is set to minimize the second minimum close approach distance (with no weight given to the first minimum

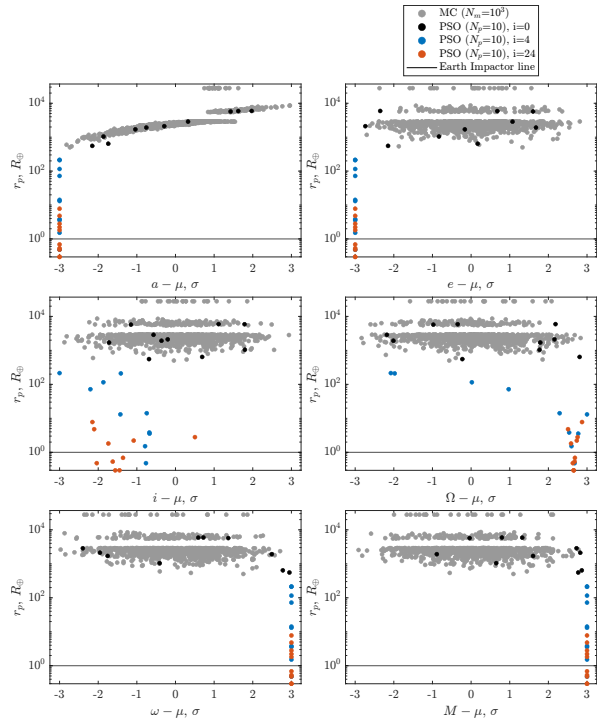


**Figure 10: Asteroid 101955 Bennu Initial Conditions**

**Table 7: Minimum Second Close Approach Distances - Bennu Case Study**

Method	Iteration	Minimum CA2, $R_{\oplus}$
MC	0	501.977
PSO	0	554.455
	1	466.288
	2	91.616
	3	44.1805
	4-5	0.4796
	6-7	0.3835
	8	0.3668
	9-13	0.2921
	14-17	0.2896
	18-20	0.2883
21-24	0.2876	

close approach distance). For the Swift-Tuttle case study, the number of samples for MC is set to 1,000 and the population of PSO is set to 25 particles and 40 generations. Figure 11 shows the optimal comet trajectory (with the minimum close approach distance to the Earth) from PSO alongside the Earth's path in the Sun-centered ecliptic J2000 frame. The comet close approaches are shown in the A-Plane in Figure 12. Unlike the other scenar-



**Table 8: Swift-Tuttle Orbital Elements at Epoch 10-Oct-1995 00:00:00 TDB**

Element	Value	Uncertainty ( $1\sigma$ )	Units
$e$	0.9632	2.9192e-4	-
$a$	3.903e9	3.119e5	km
$i$	113.454	1.714e-3	deg
$\Omega$	139.381	3.652e-4	deg
$\omega$	152.982	1.082e-3	deg
$M$	7.632	2.228e-2	deg

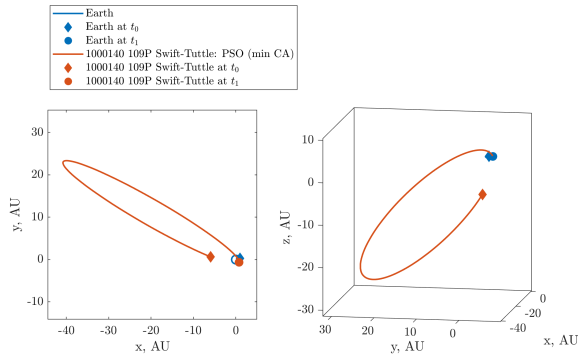


**Figure 11: Comet 101955 Swift-Tuttle Close Approach, Heliocentric Ecliptic J2000 frame**

ios where the impactor occurred at the edge of the A-Plane arrival points, due to the large uncertainty and geometry of the large period, highly eccentric comet orbit, the scatter of A-Plane points extends past the Earth impact disk in all directions. This case study illustrates the effectiveness of the PSO method for the PHO close approach problem for a newly discovered Halley-type comet with a very large uncertainty and A-Plane arrival ellipse. PSO finds an Earth impactor with a population of 25 particles and 40 iterations, whereas the 1,000 sample MC simulation only finds three minimum close approach distances interior the Earth's sphere of influence. In the comet Swift-Tuttle case study, the close approaches are again plotted with a logarithmic y-axis since the set of close approaches vary widely. In Figure 13, the PSO particles swarm down the "funnel" shape outlined by the MC and PSO initial populations and eventually find an impacting trajectory on iteration 21. Figure 13 Figure 14 shows the population of initial conditions for MC and three iterations (initial, first impact detection, and final) of PSO as the particles move towards the minimum close approach distance.

The comet case study differs from the first in that none of the initial conditions that result in an Earth-impactor are near the  $\pm 3\sigma$  boundary of the

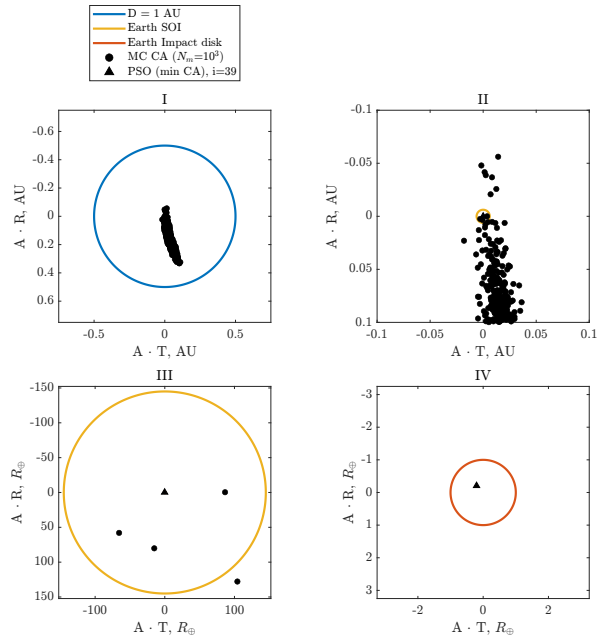


**Figure 12: Comet 109P/Swift-Tuttle A-Plane crossing**

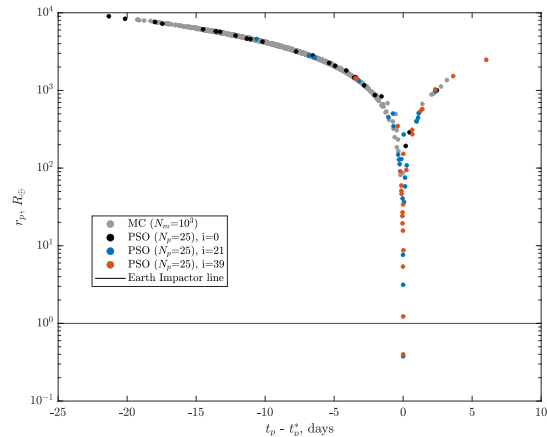


**Figure 13: Comet 109P/Swift-Tuttle Minimum Distances from Earth's center**

search space. The PSO particles find an impacting trajectory for semi-major axes near  $1.2\sigma$ , eccentricities near  $-0.5\sigma$ , inclinations at  $-2\sigma$ , right ascension of the ascending nodes near  $2.1\sigma$ , argument of periapses near  $-0.9\sigma$  and mean anomaly at  $-2.7\sigma$ . This comet Swift-Tuttle scenario verifies that PSO can find Earth impactors "hidden" in a very large uncertainty region without relying on finding extrema by searching near the boundaries of the search space.

The PHO minimum close approach distances for the Swift-Tuttle case study are shown in Table 9.

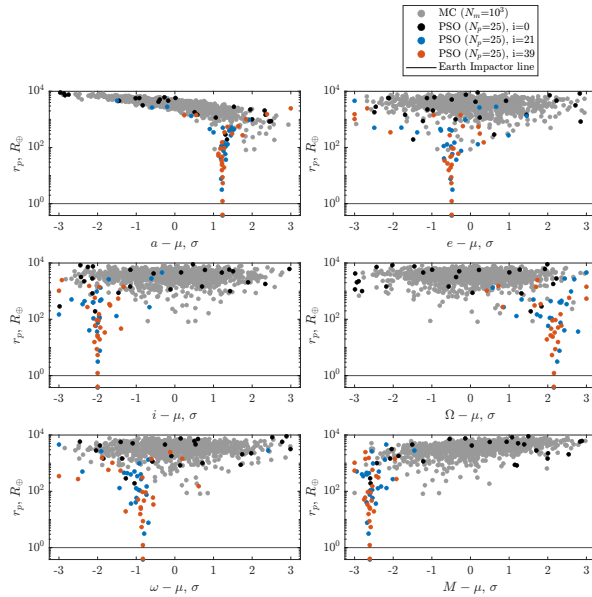


**Figure 14: Comet 109P/Swift-Tuttle Initial Conditions**

This table illustrates an example of PSO finding an impactor deeper (21 iterations) into its search process than the previous analyses.

**Table 9: Minimum Close Approach Distances - Comet Swift-Tuttle Case Study**

Method	Iteration	Minimum CA, $R_{\oplus}$
MC	0	81.5796
PSO	0	192.6312
	1	188.5704
	2	89.1325
	3	58.0195
	4-7	44.3097
	8	40.0648
	9-11	25.6319
	12	8.3909
	13-20	5.7257
	21-33	0.3775
34	0.3227	
35-39	0.2891	

**Conclusion:** Compared to the current state of the art, the introduced method outperforms existing methods both in computational efficiency and effectiveness at finding virtual impactors (VI) that are not detected with traditional statistical methods, e.g., via a Monte Carlo simulation. The presented method contributes to the global planetary defense effort by accurately and efficiently predict-

ing the “worst-case scenario” Earth close approach for a given potentially hazardous object and can be applied to other problems that are currently analyzed via statistical methods but would be better posed as optimization problems.

The authors would like to thank the 2023 IAA Planetary Defense Conference Student Grant for supporting this effort.

Note: The scenarios in this paper have been designed to illustrate the effectiveness of the proposed method for the determination of PHO minimum close approach distances, and do not represent a current best estimate of the risk to Earth posed by any PHO.

**References:** [1] S. R. Chesley (2005) *Proceedings of the International Astronomical Union* 1(S229):215–228. [2] J. D. Giorgini, et al. (2008) *Icarus* 193(1):1 ISSN 0019-1035 doi. [3] A. Milani, et al. (2002) *Asteroids III* 55 – 69. [4] B. A. Conway (Ed.) (2010) *Spacecraft Trajectory Optimization* Cambridge University Press. [5] G. Beni, et al. (1993) in *Robots and Biological Systems: Towards a New Bionics?* (Edited by P. Dario, et al.) vol. 102 703–712 Springer Berlin, Heidelberg. [6] M. Pontani, et al. (2010) *Journal of Guidance, Control, and Dynamics* 33(5):1429. [7] C. Acton, et al. (2018) *Planetary and Space Science* 150:9. [8] The SPICE Toolkit <https://naif.jpl.nasa.gov/naif/toolkit.html>. [9] R. S. Park, et al. (2021) *The Astronomical Journal* 161(3):105. [10] P. H. Cowell, et al. (1910) *Greenwich Observations in Astronomy, Magnetism and Meteorology made at the Royal Observatory, Series 2* 71:1. [11] J. E. Prussing, et al. (2013) *Orbital Mechanics* Oxford University Press 2nd edn. [12] N. Metropolis, et al. (1949) *Journal of the American Statistical Association* 44(247):335. [13] J. Kennedy, et al. (1995) *Proceedings of IEEE International Conference on Neural Networks* 1942 – 1948. [14] MATLAB R2021a <https://www.mathworks.com/help/matlab/>. [15] L. F. Shampine, et al. (1997) *SIAM Journal on Scientific Computing* 18:1.